Defining the Role of Phosphomethylethanolamine *N*-Methyltransferase from *Caenorhabditis elegans* in Phosphocholine Biosynthesis by Biochemical and Kinetic Analysis†

Lavanya H. Palavalli,‡,§ Katherine M. Brendza,§,|| William Haakenson,|| Rebecca E. Cahoon,‡ Merry McLaird,|| Leslie M. Hicks,‡ James P. McCarter,|| D. Jeremy Williams,|| Michelle C. Hresko,|| and Joseph M. Jez*,‡

Donald Danforth Plant Science Center, 975 North Warson Road, St. Louis, Missouri 63132, and Divergence, Inc., 893 North Warson Road, St. Louis, Missouri 63141

Received January 31, 2006; Revised Manuscript Received March 20, 2006

ABSTRACT: In plants and *Plasmodium falciparum*, the synthesis of phosphatidylcholine requires the conversion of phosphoethanolamine to phosphocholine by phosphoethanolamine methyltransferase (PEAMT). This pathway differs from the metabolic route of phosphatidylcholine synthesis used in mammals and, on the basis of bioinformatics, was postulated to function in the nematode *Caenorhabditis elegans*. Here we describe the cloning and biochemical characterization of a PEAMT from *C. elegans* (gene, *pmt-2*; protein, PMT-2). Although similar in size to the PEAMT from plants, which contain two tandem methyltransferase domains, PMT-2 retains only the C-terminal methyltransferase domain. RNA-mediated interference experiments in *C. elegans* show that PMT-2 is essential for worm viability and that choline supplementation rescues the RNAi-generated phenotype. Unlike the plant and *Plasmodium* PEAMT, which catalyze all three methylations in the pathway, PMT-2 catalyzes only the last two steps in the pathway, i.e., the methylation of phosphomonomethylethanolamine (P-MME) to phosphodimethylethanolamine (P-DME) and of P-DME to phosphocholine. Analysis of initial velocity patterns suggests a random sequential kinetic mechanism for PMT-2. Product inhibition by *S*-adenosylhomocysteine was competitive versus *S*-adenosylmethionine and noncompetitive versus P-DME, consistent with formation of a dead-end complex. Inhibition by phosphocholine was competitive versus each substrate. Fluorescence titrations show that all substrates and products bind to the free enzyme. The biochemical data are consistent with a random sequential kinetic mechanism for PMT-2. This work provides a kinetic basis for additional studies on the reaction mechanism of PEAMT. Our results indicate that nematodes also use the PEAMT pathway for phosphatidylcholine biosynthesis. If the essential role of PMT-2 in *C. elegans* is conserved in parasitic nematodes of mammals and plants, then inhibition of the PEAMT pathway may be a viable approach for targeting these parasites with compounds of medicinal or agronomic value.

Phosphatidylcholine is a major phospholipid component in the cellular membranes of eukaryotes (*1*−*4*). The biosynthesis of phosphatidylcholine in various organisms occurs through three different metabolic pathways (Figure 1). The de novo choline or Kennedy pathway, in which choline is converted into phosphatidylcholine, provides the major synthetic route in mammals, fungi, and bacteria (*1*−*4*). Yeast and mammalian liver cells use the CDP-diacylglycerol pathway, which begins with formation of phosphatidylserine from serine and CDP-diacylglycerol (*4*−*6*). Following the conversion of phosphatidylserine to phosphatidylethanolamine, the subsequent addition of methyl groups derived from *S*-adenosylmethionine (SAM)[1] to phosphatidylethanolamine yields phosphatidylcholine. In plants, the methylation of phosphoethanolamine accounts for nearly all the metabolic flux to phosphocholine, and subsequently to phosphatidylcholine via the Kennedy pathway (*7*−*12*). In this pathway, phosphoethanolamine is sequentially methylated to phosphomonomethylethanolamine (P-MME), phosphodimethylethanolamine (P-DME), and phosphocholine. Phosphocholine then enters the Kennedy pathway. Recent studies indicate that the protozoan parasite *Plasmodium falciparum* (the causative agent of malaria) synthesizes phosphatidylcholine using a plant-like phosphoethanolamine methylation pathway (*13*, *14*).

S-Adenosyl-L-methionine:phosphoethanolamine *N*-methyltransferase (PEAMT, EC 2.1.1.103) catalyzes the conversion of phosphoethanolamine to P-MME, P-MME to P-DME,

† This work was supported by a grant from the Environmental Protection Agency (X-83228201) to J.P.M., D.J.W., M.C.H., and J.M.J.

* To whom correspondence should be addressed. Phone: (314) 587-1450. Fax: (314) 587-1550. E-mail: jjez@danforthcenter.org.

‡ Donald Danforth Plant Science Center.

§ These authors contributed equally to this work.

|| Divergence, Inc.

[1] Abbreviations: dsRNA, double-stranded RNA; ESI-QTOF, electrospray ionization quadrupole time-of-flight; GFP, green fluorescent protein; IPTG, isopropyl 1-thio-β-D-galactopyranoside; NGM, nematode growth medium; NTA, nitriloacetic acid; PEAMT, *S*-adenosyl-L-methionine:phosphoethanolamine *N*-methyltransferase; P-MME, phosphomonomethylethanolamine; P-DME, phosphodimethylethanolamine; PMT-2, *C. elegans S*-adenosyl-L-methionine:phosphomethylethanolamine *N*-methyltransferase; RNAi, RNA-mediated interference; SAH, *S*-adenosylhomocysteine; SAM, *S*-adenosyl-L-methionine; TLC, thin-layer chromatography.

10.1021/bi060199d CCC: $33.50
Published on Web 04/22/2006

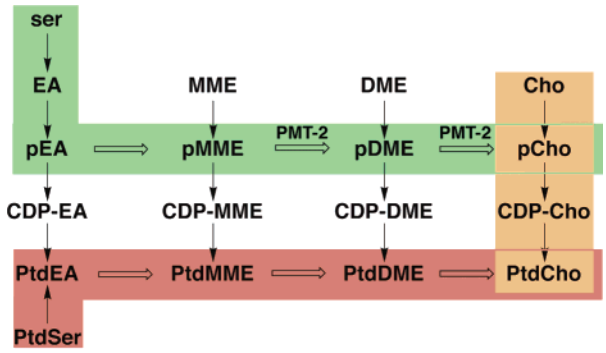

FIGURE 1: Overview of phosphatidylcholine biosynthesis in mammals, fungi, bacteria, plants, apicomplexans, and nematodes. Metabolites in the de novo choline or Kennedy pathway for phosphatidylcholine (PtdCho) synthesis are indicated with the orange box. The CDP-diacylglycerol pathway (red box) is shown beginning with phosphatidylserine (PtdSer). The phosphobase methylation pathway found in plants and nematodes is highlighted with the green box. Phosphocholine (pCho) is then converted into PtdCho by the Kennedy pathway. Horizontal arrows denote methylation reactions, with the two steps catalyzed by PMT-2 from *C. elegans* indicated. In vivo conversions between the base, phosphobase, CDP, and phospholipid substrates are shown as vertical arrows. Metabolite names consist of a prefix (p, phospho; CDP, cytidine 5′-diphosphate; Ptd, phosphatidyl) and a core name (EA, ethanolamine; MME, monomethylethanolamine; DME, dimethylethanolamine; Cho, choline).

and P-DME to phosphocholine. The genes for PEAMT from *Arabidopsis thaliana* (thale cress), *Spinacia oleracea* (spinach), and *Triticum aestivum* (wheat) encode proteins containing two tandem methyltransferase domains (*10*−*12*). The N-terminal methyltransferase domain catalyzes the methylation of phosphoethanolamine to P-MME, and the C-terminal domain converts P-MME to P-DME and P-DME to phosphocholine (*11*, *12*). In contrast to the plant enzymes, functional analysis of the PEAMT from *P. falciparum* indicates that one methyltransferase domain performs all three methylation reactions at a single active site (*13*, *14*). Earlier studies reported the presence of ESTs in the free-living nematode *Caenorhabditis elegans* that share sequence similarity with the plant and *P. falciparum* PEAMT (*11*−*13*). This suggests that nematodes also use the plant-like pathway for phosphatidylcholine biosynthesis, but the physiologic function of these PEAMT-like proteins from any nematode remains unexamined.

Since the *Plasmodium* and nematode PEAMT lack sequence homology with the phosphatidylethanolamine methyltransferases from other eukaryotes and the mammalian genomes contain no PEAMT homologues (*13*), the role of PEAMT in phospholipid biosynthesis in these organisms provides a potential target for the development of antiprotozoan and anthelmithic compounds with medical and agricultural uses (*15*, *16*). In *P. falciparum*, the phospholipid content increases upon infection with phosphatidylcholine comprising half of the phospholipid pool (*17*). Previous work shows that phospholipid and phosphocholine analogues can inhibit *P. falciparum* membrane biogenesis and retard growth (*13*, *18*−*21*).

Currently, information about the biochemical and kinetic properties of the PEAMT from any source is limited. Understanding the kinetic and chemical reaction mechanisms of PEAMT is essential for the development of inhibitors targeting this enzyme. Here we describe the cloning, in vivo analysis by RNA-mediated interference, and kinetic examination of a *C. elegans* PEAMT that catalyzes the methylations of P-MME to P-DME and P-DME to phosphocholine. Using a combination of initial velocity studies and analysis of product inhibition profiles, we show that the enzyme follows a random bi-bi kinetic mechanism. This work provides a kinetic basis for further studies on the reaction mechanism of PEAMT and the development of PEAMT-specific inhibitors.

EXPERIMENTAL PROCEDURES

Materials. Escherichia coli Rosetta 2 (DE3) pLysS cells were purchased from Novagen. Ni^{2+}−nitrilotriacetic acid (NTA)−agarose beads were obtained from Qiagen. The HiTrap Q-Sepharose and HiLoad 26/60 Superdex-200 FPLC columns were from Amersham Biosciences. Radiolabeled [*methyl*-^{14}C]SAM (55.8 mCi/mmol) was bought from either American Radiochemicals or Amersham Biosciences. P-MME and P-DME were synthesized by Gateway Chemical, Inc. All other reagents were from either Sigma-Aldrich or Research Products International and were of ACS reagent quality or better.

Cloning of pmt-2 and Generation of the Expression Vector. The *pmt-2* coding region (GenBank accession number AAB04824.1; wormbase locus F54D11.1)[2] was amplified by PCR from a *C. elegans* EST (cDNA; Genome Sequencing Center at Washington University School of Medicine, St. Louis, MO) using 5′-dGAGGAATTCCAT**ATG**TCATCTC-TATCCATTCC-3′ as the forward primer (NdeI site underlined; coding region start codon in bold) and 5′-dGGAT-TCGAGCTC**TTA**TTTTGGGAATGGTTTTTG-3′ as the reverse primer (SacI site underlined; coding region stop codon in bold). The 1.3 kb PCR product was gel-extracted (QIAquick Spin Gel Extraction Kit, Qiagen, Inc.) and subcloned into the pCRII-TOPO vector (Invitrogen). Automated nucleotide sequencing confirmed the fidelity of the PCR product. Digesting the pCRII-TOPO-CePMT-2 vector with NdeI and SacI and then ligating the 1.3 kb DNA fragment into NdeI/SacI-digested pET28a yielded the pET28a-*pmt-2* expression vector.

RNA-Mediated Interference (RNAi) of pmt-2 by Feeding and Chemical Rescue in C. elegans. For RNAi in *C. elegans*, a double-stranded RNA (dsRNA) molecule was delivered by raising feeding worms on *E. coli* engineered to produce the dsRNA molecule (*22*, *23*). An 854-nucleotide fragment was amplified from the *pmt-2* gene using oligonucleotide primers (5′-dCCAGATTATTACCAACGCCG-3′ and 5′-dTGAACTTACATAGATTCTTG-3′). The *pmt-2* genomic fragment was cloned into the L4440 vector (*24*) between opposing T7 polymerase promoters. The vector was then

[2] Since the protein encoded by this cDNA (GenBank accession number AAB04824.1; wormbase locus, F54D11.1) catalyzes the last two methylation reactions in phosphocholine biosynthesis, it should be designated *S*-adenosyl-L-methionine:phosphomethylethanolamine *N*-methyltransferase. According to the guidelines for gene and protein nomenclature for *C. elegans* (http://www.cbs.umn.edu/CGC/Nomenclature/nomenguid.htm), this gene is now designated *pmt-2* and the protein named PMT-2. The protein catalyzing the initial methylation of phosphoethanolamine should be termed *S*-adenosyl-L-methionine: phosphoethanolamine *N*-methyltransferase. The *C. elegans* PEAMT (GenBank accession number AAA81102.1; wormbase locus, ZK622.3a/3b) that catalyzes this reaction is designated PMT-1 and the gene *pmt-1*, and they will be described elsewhere.

transformed into *E. coli* strain HT115, which contains the gene for the T7 RNA polymerase. Control *C. elegans* were fed *E. coli* transformed with the L4440 vector encoding green fluorescent protein (GFP). Feeding RNAi was initiated from *C. elegans* larva at 20 °C on nematode growth medium (NGM)−agar plates containing 2.5 mg/mL isopropyl 1-thio-β-D-galactopyranoside (IPTG) and *E. coli* expressing either *pmt-2* or control GFP dsRNA.

For chemical rescue of the *pmt-2* RNAi-generated phenotype, ethanolamine, monomethylethanolamine, dimethylethanolamine, or choline was incorporated into the NGM−agar plates at various concentrations before the plates were poured. The plates were seeded with *E. coli* expressing dsRNA homologous to *pmt-2*. In one set of experiments, either a first-stage larva (L1) or a dauer larva was placed on each plate and the P0 and F1 progeny were examined for 5 days. The dauer larva were *daf-7(e1372)* mutants, which are constituitive dauers at 25 °C but are wild-type at 20 °C. Upon placing the dauers on the RNAi-feeding plates, the incubation temperature was shifted from 25 °C to 20 °C to induce the worms to exit dauer and start feeding. In a second set of experiments, a single stage-four (L4) *C. elegans* hermaphrodite was placed on each plate and allowed to lay eggs for 24 h. The phenotype of the P0 and the F1 progeny was scored 48 h and 72 h after the initial 24 h egg-laying period.

Expression in E. coli and Protein Purification. The pET28a-*pmt-2* expression construct was transformed into *E. coli* Rosetta 2 (DE3) pLysS cells. Transformed *E. coli* were grown at 30 °C in Terrific Broth containing 50 μg/mL kanamycin and 35 μg/mL chloramphenicol until the A_{600} reached ~0.8−1.2. Following induction with 1 mM IPTG, the cultures were grown at 25 °C for 4−6 h. Cells were harvested by centrifugation (10000*g* for 10 min) and resuspended in lysis buffer [50 mM Tris (pH 8.0), 500 mM NaCl, 25 mM imidazole, 10% (v/v) glycerol, and 1% (v/v) Tween 20]. After sonication and centrifugation (50000*g* for 1 h), the supernatant was loaded onto a Ni^{2+}−NTA column previously equilibrated with lysis buffer. The column was washed with wash buffer (lysis buffer without Tween 20). Bound protein was eluted using elution buffer (wash buffer containing 250 mM imidazole). Eluted protein was buffer exchanged into 50 mM Tris (pH 8.0) and 100 mM NaCl and loaded onto a HiTrap Q-Sepharose FPLC column. A linear salt gradient (from 100 to 500 mM NaCl) was used to elute protein from the column. Fractions containing PMT-2 were pooled and loaded onto a Superdex-200 size-exclusion FPLC column equilibrated in 25 mM Hepes (pH 7.5) and 100 mM NaCl. Fractions with PMT-2 were pooled, concentrated to 15 mg/mL, and stored at −80 °C. Protein concentrations were determined by the Bradford method (protein assay, Bio-Rad) with bovine serum albumin as the standard.

Enzyme Assays. A radiochemical assay was used to measure enzymatic activity (*4*). Standard assay conditions were 0.1 M Hepes·KOH (pH 8), 2 mM Na_2EDTA, 10% glycerol (v/v), 2.5 mM SAM (100 nCi of [*methyl*-^{14}C]SAM), and 10 mM P-DME in 100 μL. Assays contained 0.5 μg of protein and were incubated for 2.5, 5, and 7 min at 30 °C. The amount of protein and the time of reaction provided a linear rate of product formation. Reactions were terminated by addition of 1 mL of ice-cold water. The phosphorylated product was purified by loading the quenched reaction to a 1 mL Dowex (50WX8-100)-resin column, which was washed with 2 mL of ice-cold water and then eluted with 10 mL of 0.1 N HCl. For scintillation counting, 2 mL of the eluant was mixed with 3 mL of Ecolume scintillation fluid.

Steady-state kinetic parameters for SAM (15−2500 μM) were determined under standard assay conditions at either 10 mM P-DME or 20 mM P-MME. Product formation was assessed by scintillation counting. The k_{cat} and K_m values of PMT-2 for P-DME and P-MME (0.25−20 mM) were determined at 2.5 mM SAM. All data were fit to the Michaelis−Menten equation [$v = (k_{cat}[S])/(K_m + [S])$] using Kaleidagraph (Synergy Software).

Characterization of Reaction Products. Thin-layer chromatography (TLC) and electrospray ionization quadrupole time-of-flight (ESI-QTOF) mass spectrometry were used to confirm the chemical identity of the reaction products. For confirmation of reaction product identities by TLC, PMT-2 was assayed under the standard reaction conditions containing 400 nCi of [*methyl*-^{14}C]SAM and 10 mM phosphoethanolamine, P-MME, or P-DME (*4*, *7*). Reaction products were purified as described above, collected, and evaporated to dryness. The dry product was resuspended in methanol and applied to a Whatman LK6D silica TLC plate, which was then developed with an *n*-butanol/methanol/concentrated HCl/water mixture (7.5:7.5:1:1; v/v/v/v). Phosphorimaging was used to visualize the radiolabeled products. Migration of reaction products was compared to that of authentic standards.

To determine the chemical identity of reaction products (i.e., P-DME and phosphocholine) by ESI-QTOF mass spectrometry, standard reactions were performed without incorporation of radiolabeled SAM. Reaction products were purified as described above, collected, and evaporated to dryness. Samples were resuspended in 100 μL of 10% (v/v) acetonitrile and analyzed with an ABI QSTAR XL (Applied Biosystems/MDS Sciex) hybrid QTOF MS/MS mass spectrometer equipped with a nanoelectrospray source (Protana XYZ manipulator). Positive mode nanoelectrospray was generated from borosilicate nanoelectrospray needles at 1.5 kV. TOF MS spectra were obtained using Analyst QS software with an *m*/*z* range of 30−500. The observed *m*/*z* values of the parent ion and fragmentation pattern for each product [neutral loss of HPO_3 (80 Da) and H_3PO_4 (98 Da)] were determined: P-DME, $[M + H]^+$ 170.07, $[(M - HPO_3) + H]^+$ 90.10, $[(M - H_3PO_4) + H]^+$ 72.09; phosphocholine, [M] 184.08, $[M - HPO_3]$ 104.12, $[M - H_3PO_4]$ 86.10. The parent ion and fragmentation pattern of the products matched those obtained using standards: P-DME, $[M + H]^+$ 170.06, $[(M - HPO_3) + H]^+$ 90.09, $[(M - H_3PO_4) + H]^+$ 72.08; phosphocholine, [M] 184.08, $[M - HPO_3]$ 104.11, $[M - H_3PO_4]$ 86.10.

Analysis of the Bisubstrate Kinetic Mechanism. Analysis of the kinetic mechanism of PMT-2 used global fitting analysis (*25*−*28*). Reaction rates were measured under standard assay conditions with a matrix of substrate concentrations (15−2500 μM SAM and 0.25−20 mM P-DME). Global curve fitting in SigmaPlot (Systat Software, Inc.) was used to model the kinetic data to rapid equilibrium rate equations describing ping-pong [$v = (V_{max}[A][B])/(K_B[A] + K_A[B] + [A][B])$], ordered sequential [$v = (V_{max}[A][B])/(K_AK_B + K_B[A] + [A][B])$], and random sequential [$v = (V_{max}[A][B])/(\alpha K_AK_B + K_B[A] + K_A[B] + [A][B])$], kinetic

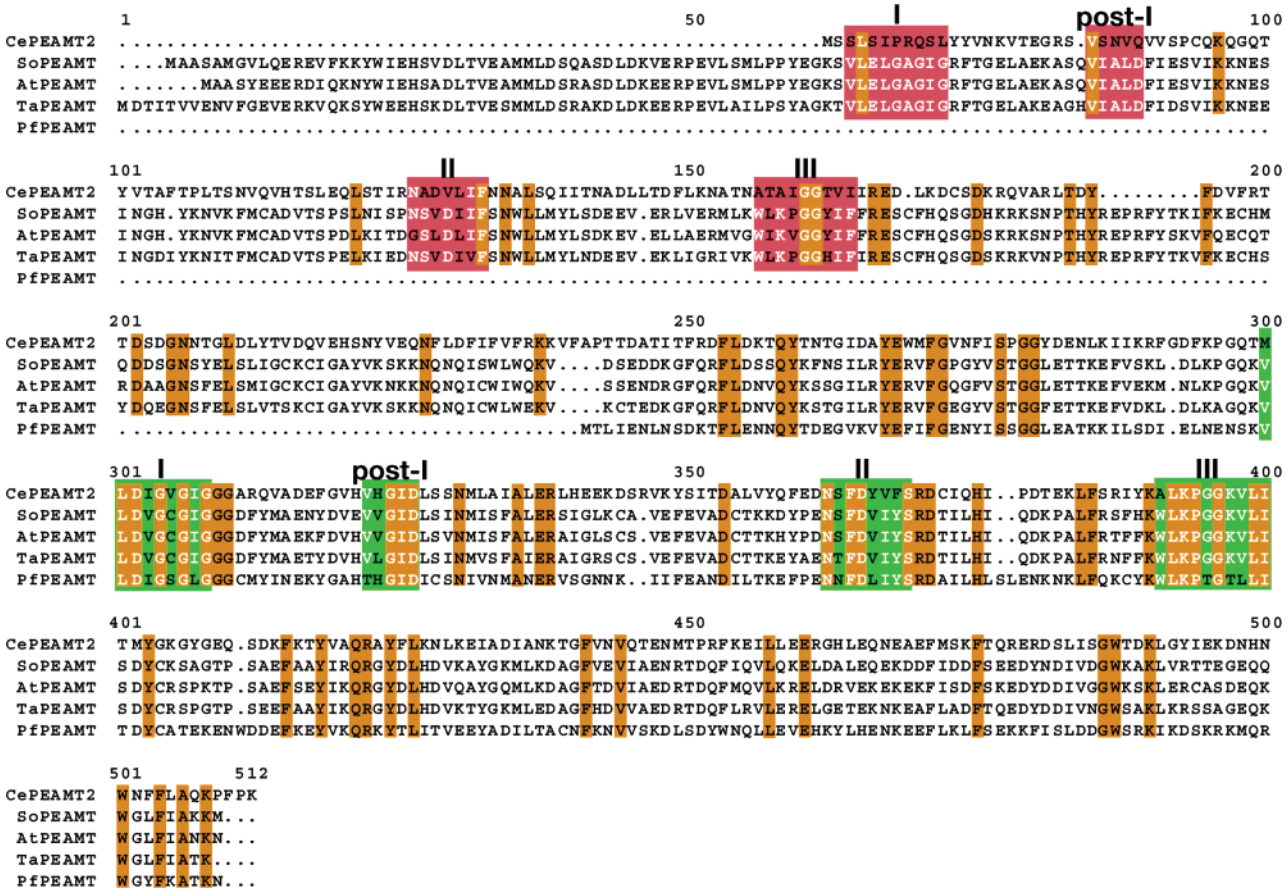

FIGURE 2: Amino acid sequence comparison of PEAMT. Multiple-sequence comparison of the *C. elegans* PMT-2 (CePEAMT2, AAB04824.1), *S. oleracea* (spinach) PEAMT (SoPEAMT, AAF61950.1), *T. aestivum* (wheat) PEAMT (TaPEAMT, AAL40895.1), *Ar. thaliana* (thale cress) PEAMT (AtPEAMT, AAG41121.1), and *P. falciparum* PEAMT (PfPEAMT, AAR08195.1). Invariant amino acids are highlighted with orange boxes. Sequence motifs defining the methyltransferase domains are labeled I, post-I, II, and III. The motifs in the first and second methyltransferase domains are denoted with red and green boxes, respectively. Highly conserved positions within the methyltransferase sequence motifs are shown with white letters. Sequence alignment was performed using the Multalin website (http://prodes.toulouse.inra.fr/multalin/multalin.html).

mechanisms, where v is the initial velocity, V_{max} is the maximum velocity, K_A and K_B are the K_m values for substrates A and B, respectively, and α is the interaction factor if the binding of one substrate changes the dissociation constant for the other substrate (*29*).

Product Inhibition Assays. Reaction rates of PMT-2 in the presence of *S*-adenosylhomocysteine (SAH) or phosphocholine were determined radiometrically under standard assay conditions. Enzymatic activity was measured in reaction mixtures containing inhibitor, either SAH (10−500 μM) or phosphocholine (0.5−6 mM), and varied concentrations of SAM (15−2500 μM) or P-DME (0.25−20 mM). The global fitting analysis of data from inhibition experiments used SigmaPlot to fit all data to the equations for competitive ($v = (V_{max}[S])/\{[K_m(1 + [I]/K_{is}) + [S]]\}$) or noncompetitive ($v = (V_{max}[S])/\{[K_m(1 + [I]/K_{is})] + [[S](1 + [I]/K_{ii})]\}$) inhibition (*30*).

Fluorescence Titration of Ligand Binding. Fluorescence emission spectra were measured from 300 to 500 nm (slit width of 5 nm) with an excitation wavelength of 295 nm (slit width of 5 nm) using a Varian Cary spectrofluorometer. The final buffer used for ligand titrations contained 100 mM Hepes·KOH (pH 8.5), 2 mM EDTA, and 200 μg of protein. Compounds used for titration experiments were SAM (0−10 mM), P-DME (0−20 mM), phosphocholine (0−40 mM), and SAH (0−250 μM). To calculate the K_d based on signal intensity, data were fitted to a reversible two-state model of binding

$$\Delta F = (\Delta F_{max}[L])/([L] + K_d)$$

where ΔF is the change in fluorescence in the presence of ligand (L) and ΔF_{max} is the maximal change in signal. The data were also plotted as a linear transform of the same equation in which the slope yields K_d (R vs R/[L]), where R is the change in fluorescence.

RESULTS

Analysis of the pmt-2 cDNA from C. elegans. A full-length cDNA encoding a polypeptide (*C. elegans* hypothetical protein AAB04824.1) similar in sequence to the PEAMT from *Plasmodium*, spinach, wheat, and *Arabidopsis* was isolated (*10*−*13*). The cDNA of 1311 bp contains an open reading frame for a 437-amino acid polypeptide with a calculated molecular mass of 49.8 kDa and a pI of 5.6. The predicted amino acid sequence is 30.4, 30.7, and 29.5% identical with those of the spinach, wheat, and *Arabidopsis* PEAMT, respectively, over the length of the PMT-2 protein sequence and 73.3% identical with the smaller (266-amino acid) *Plasmodium* PEAMT, primarily in the C-terminal region of the *C. elegans* protein (Figure 2). In addition, ESTs sharing 30−40% sequence identity with PMT-2 appear in

Table 1: Summary of *C. elegans pmt-2* Feeding RNAi and Chemical Rescue Phenotypes[a]

starting worm (P0)	added compound	phenotype
L1	none	P0 sterility
L1	10 or 30 mM EA, MME, or DME	P0 sterility
L1	10 mM choline	P0 sterility
L1	30 mM choline	fertile adults
dauer	none	P0 sterility
dauer	10 or 30 mM EA, MME, or DME	P0 sterility
dauer	10 mM choline	P0 sterility
dauer	30 mM choline	fertile adults
L4	none	F1 L1/L2 arrest; lethality
L4	10 or 30 mM EA, MME, or DME	F1 L1/L2 arrest; lethality
L4	10 mM choline	F1 L1/L2 arrest; lethality
L4	30 mM choline	wild-type F1

[a] *C. elegans* at the L1, dauer, or L4 stage were placed on NGM−agar plates containing the indicated compound (EA, ethanolamine; MME, monomethylethanolamine; DME, dimethylethanolamine), as described in Experimental Procedures. The observed phenotypes are indicated.

plant parasitic nematodes (*Meloidogyne javanica*, *Meloidogyne chitwoodi*, *Meloidogyne incognita*, and *Globodera rostochiensis*) and mammalian parasitic nematodes (*Ascaris suum* and *Ancylostoma ceylanicum*).

Alignment of the plant, *Plasmodium*, and *C. elegans* PEAMT amino acid sequences revealed differences in the organization of the methyltransferase domains (Figure 2). The plant PEAMTs contain two tandem methyltransferase domains defined by a set of consensus sequence motifs termed I, post-I, II, and III (*31*). In the plant enzymes, the first domain methylates phosphoethanolamine to P-MME and the second domain catalyzes the two methylation reactions leading to phosphocholine (*10*−*12*). The *Plasmodium* PEAMT, the sequence of which is similar with the C-terminal half of PMT-2, consists of a single methyltransferase domain capable of all three methylation reactions (*13*). Although PMT-2 is similar in amino acid length to the plant enzymes, comparison of the methyltransferase consensus motifs in the N- and C-terminal domains suggests that PMT-2 contains only the C-terminal methyltransferase domain, since the N-terminal I, post-I, II, and III motifs lack a high degree of sequence similarity with the plant enzymes. In addition, the functionally important Gly-X-Gly-X-Gly sequence located in N-terminal motif I is missing from PMT-2 (*32*). These sequence comparisons suggest that PMT-2 does not catalyze the methylation of phosphoethanolamine.

RNAi of pmt-2 by Feeding and Chemical Rescue in C. elegans. RNAi was used to probe the function of PMT-2 in *C. elegans* (Table 1). A dsRNA construct was designed to inactivate the *pmt-2* gene and was delivered by raising feeding nematodes on *E. coli* producing the dsRNA corresponding to either *pmt-2* or GFP (control). In all the control experiments, normal development was observed. With bacteria expressing the dsRNA corresponding to *pmt-2*, if the parental worm (P0) was either an L1 or a *daf-7* (see Experimental Procedures), then the phenotype was complete or highly penetrant (>95%) P0 sterility. If the parental nematode was an L4 larva, the observed phenotype was arrested development and lethality in the progeny (F1) L1/L2 larva. These experiments show that *C. elegans* grown in the presence of *E. coli* expressing dsRNA from the *pmt-2* gene were developmentally impaired, indicating that the gene

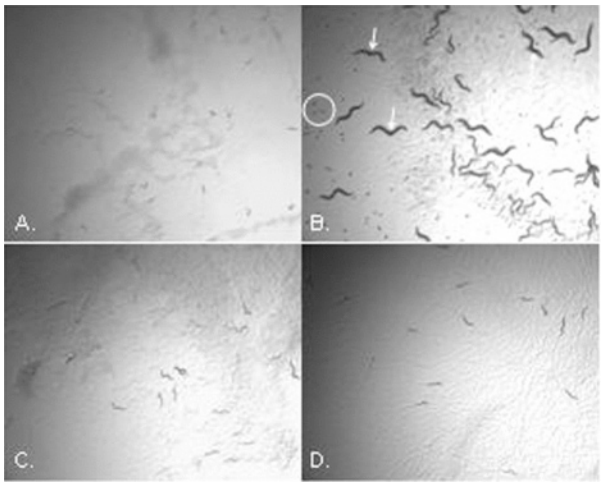

FIGURE 3: Chemical rescue of the *pmt-2* RNAi phenotype with pathway intermediates. Individual *C. elegans* L4 hermaphrodites were placed on NGM−agar plates containing bacteria producing *pmt-2* dsRNA and (A) no additional compounds, (B) 30 mM choline, (C) 10 mM DME, or (D) 30 mM DME. Photographs show the phenotype of the F1 progeny 4 days after introduction of the original L4 to the plate. (A) F1 progeny have arrested development at the L1 stage. (B) F1 progeny have developed to fertile adults (arrows) and produced F2 eggs (circle) and larvae. (C and D) F1 progeny have arrested development and no F1 adults are present.

provides an essential function in multiple developmental steps in *C. elegans*.

To test whether the RNAi-generated phenotype could be rescued by providing metabolites, *C. elegans* were fed *E. coli* expressing dsRNA homologous to either *pmt-2* or GFP (control) on standard media or media supplemented with ethanolamine, monomethylethanolamine, dimethylethanolamine, or choline (Figure 3). The free base forms of the metabolites were used to facilitate uptake into the worms and subsequent conversion to the corresponding phosphobases by endogenous ethanolamine and choline kinases (*33*). In the control experiments using GFP, nematodes (L1, dauer, and L4) developed normally on either standard or supplemented media. As summarized in Table 1, providing ethanolamine, monomethylethanolamine, or dimethylethanolamine did not reverse the RNAi-generated phenotype for the L1, dauer, or L4 worms; however, addition of 30 mM choline rescued the P0 sterility and F1 larval arrest associated with the *pmt-2* RNAi-generated phenotype (Figure 3B).

Expression, Purification, and Substrate Preference of PMT-2. Hexahistidine-tagged PMT-2 was expressed in *E. coli* and purified using Ni^{2+}-affinity, anion-exchange, and size-exclusion chromatography (Figure 4A). Purified recombinant PMT-2 migrated with a molecular mass of ~50 kDa on SDS−PAGE, which corresponds to the predicted mass of the His-tagged protein (51.9 kDa). Size-exclusion chromatography of PMT-2 indicated that the protein migrates as a 46 kDa species, corresponding to a physiologic monomer, which is similar to the result reported for the PEAMT from spinach (*11*).

To verify the predicted activity of PMT-2, purified protein was assayed with phosphoethanolamine, P-MME, and P-DME (Figure 4B). These experiments showed that the *C. elegans* enzyme efficiently catalyzes the last two methylation reactions in phosphocholine synthesis, but not the initial methylation of phosphoethanolamine. In addition, the reac-

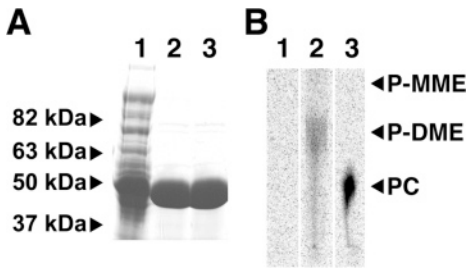

FIGURE 4: Protein expression and substrate specificity of PMT-2. (A) SDS−PAGE samples were stained for total protein using Coomassie Blue. Arrows correspond to the indicated molecular mass markers. Lanes 1−3 show the purification of PMT-2 as follows: (1) sonicate (75 μg of protein); (2) Ni^{2+}−NTA purified protein (10 μg of protein), and (3) final size-exclusion purified protein (10 μg of protein). (B) TLC analysis of the PMT-2 reaction products. PMT-2 (1 μg) was incubated for 5 min with radiolabeled SAM and either phosphoethanolamine (lane 1), P-MME (lane 2), or P-DME (lane 3). Products were isolated as described in Experimental Procedures. Positions of P-MME, P-DME, and phosphocholine (PC) standards are indicated at the right.

Table 2: Steady-State Kinetic Parameters[a]

substrate	k_{cat} (min^{-1})	K_m (mM)	k_{cat}/K_m (M^{-1} s^{-1})
SAM	494 ± 32	0.27 ± 0.06	29400
P-DME	587 ± 16	1.19 ± 0.12	8220
P-MME	565 ± 27	3.34 ± 0.46	2820

[a] Reactions were performed using a radiometric assay as described in Experimental Procedures. Kinetic parameters for SAM were determined at 10 mM P-DME. All k_{cat} and K_m values are expressed as the mean ± the standard error ($n = 3$).

tion products generated by PMT-2 from P-MME and P-DME were confirmed as P-DME and phosphocholine, respectively, by ESI-QTOF mass spectrometry as described in Experimental Procedures. In the presence of SAM, PMT-2 exhibited specific activities of 550 and 370 nmol of product min^{-1} (mg of protein)$^{-1}$ for P-DME and P-MME, respectively. A limited activity of 5 nmol of product min^{-1} (mg of protein)$^{-1}$ was observed using phosphoethanolamine and SAM as substrates.

Steady-State Kinetic Analysis. The steady-state kinetic parameters (k_{cat} and K_m) of PMT-2 for SAM, P-MME, and P-DME were determined using a radiometric assay (Table 2). When the enzyme was assayed with either phosphobase as a substrate, the k_{cat} and K_m values of the enzyme for SAM were similar. Compared to those of the spinach, wheat, and *Plasmodium* enzymes (*11*−*13*), the K_m of PMT-2 for SAM is 2−5-fold higher; however, previous analysis of the other PEAMT used phosphoethanolamine, which is not a substrate of PMT-2. Thus, no kinetic data have been previously reported for P-MME and P-DME with a PEAMT from any species. The difference in K_m for SAM likely reflects the substrate specificity of PMT-2. In addition, the turnover rates of the *C. elegans* enzyme are ~500-fold higher than those reported for the PEAMT from *Plasmodium* (*13*).

Table 3: Kinetic Constants for a Random Sequential Bi-Bi Kinetic Model[a]

fitted parameters	
V_{max} [nmol min^{-1} (mg of protein)$^{-1}$]	555 ± 19
K_{SAM} (mM)	0.66 ± 0.05
K_{P-DME} (mM)	4.56 ± 0.38
α	0.30 ± 0.09
calculated values	
αK_{SAM} (mM)	0.20
αK_{P-DME} (mM)	1.4

[a] K_{SAM} and K_{P-DME} are the equilibrium dissociation constants for the binding of SAM and P-DME, respectively, to the enzyme. α is the interaction factor between the substrates.

Initial Velocity Studies of the Kinetic Mechanism. Three possible kinetic mechanisms, i.e., ping-pong, ordered sequential, and random sequential, describe the possible two-substrate to two-product (bi-bi) reactions (*29*). To distinguish between these different kinetic models for PMT-2, reaction rates were determined using a matrix of SAM and P-DME concentrations (*29*, *30*, *34*). Use of P-DME eliminated potential complications arising from the product of the first methylation reaction being used as a substrate in the second methylation reaction. The resulting data (Figure 5) were simultaneously fit to the equations describing the potential bi-bi kinetic mechanisms. Examination of Lineweaver−Burk plots, residual errors, the standard error of the fitted parameters, and the correlation coefficient of the fit determined the quality of the fit.

The kinetic data showed that all the initial velocity line patterns intersected, indicating that the kinetic mechanism is not a ping-pong type. The best fit of the data, shown as lines in Figure 5, was to a random sequential mechanism ($r^2 = 0.997$), which was better than the fit to an ordered sequential ($r^2 = 0.969$) mechanism. The fitted kinetic parameters are summarized in Table 3. On the basis of this analysis, the binding of either SAM or P-DME increases the binding affinity for the other substrate approximately 3-fold

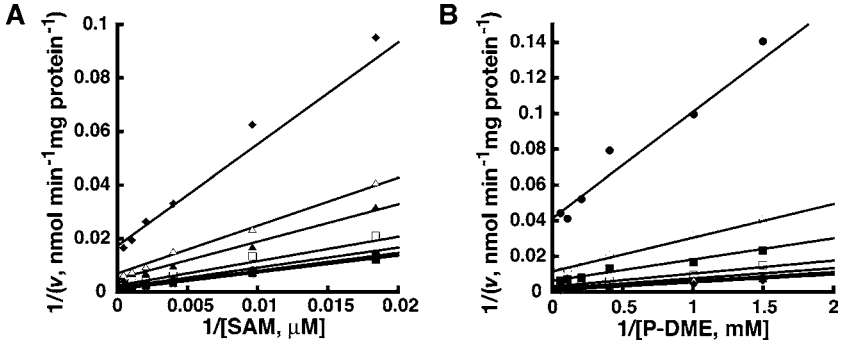

FIGURE 5: Initial velocity variation of substrates. Experimental data are indicated by the symbols in the double-reciprocal plots of the substrate variation experiments. The lines shown represent the global fits of all data to the equation for a random sequential bi-bi mechanism ($r^2 = 0.997$). Assays were performed as described in Experimental Procedures. (A) Double-reciprocal plot of $1/v$ vs 1/[SAM] at 0.25, 0.67, 1.0, 2.5, 5.0, 10, and 20 mM P-DME (from top to bottom). (B) Double-reciprocal plot of $1/v$ vs 1/[P-DME] at 15, 50, 100, 250, 500, 1000, and 2500 μM SAM (from top to bottom).

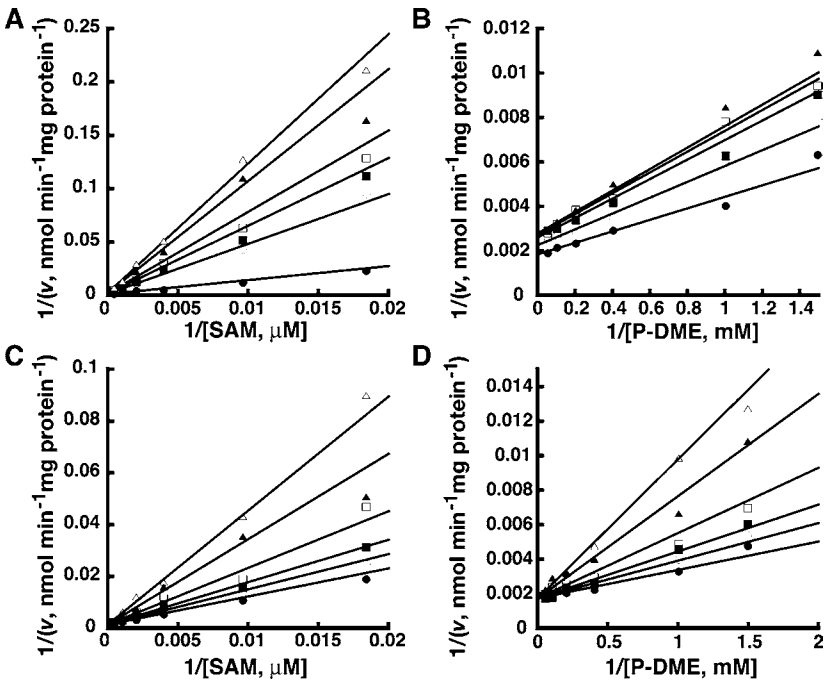

FIGURE 6: Product inhibition studies. Product inhibition assays were performed as described in Experimental Procedures. The lines show the fit to the data. (A) Double-reciprocal plot of $1/v$ vs 1/[SAM] at 0, 37, 67, 100, 250, and 500 μM *S*-adenosylhomocysteine (SAH) (from top to bottom). (B) Double-reciprocal plot of $1/v$ vs 1/[P-DME] at 0, 37, 67, 100, 250, and 500 μM SAH (from top to bottom). (C) Double-reciprocal plot of $1/v$ vs 1/[SAM] at 0, 0.5, 1, 2, 4, and 6 mM phosphocholine (from top to bottom). (D) Double-reciprocal plot of $1/v$ vs 1/[P-DME] at 0, 0.5, 1, 2, 4, and 6 mM phosphocholine (from top to bottom).

Table 4: Product Inhibition Patterns[a]

varied substrate	inhibitor	fixed substrate	inhibition	K_{is} (μM)	K_{ii} (μM)
SAM	SAH	P-DME (10 mM)	C	9.8 ± 1.2	
P-DME	SAH	SAM (2.5 mM)	NC	8.4 ± 1.7	12.6 ± 1.4
SAM	PC	P-DME (10 mM)	C	1960 ± 210	
P-DME	PC	SAM (2.5 mM)	C	1540 ± 268	

[a] All assays ($n = 3$) were performed as described in Experimental Procedures. The inhibition patterns are as follows: C, competitive; NC, noncompetitive. PC is phosphocholine.

($\alpha = 0.30$). The model-derived values of αK_{SAM} and αK_{P-DME} (Table 3) were comparable to the K_m values of each substrate shown in Table 2.

Product Inhibition Studies. To distinguish between random sequential and ordered sequential mechanisms for PMT-2, product inhibition studies were performed (*30*, *35*). Product inhibition by SAH versus SAM and P-DME showed competitive and noncompetitive inhibition patterns, respectively (Figure 6A,B). Fitting of the SAH inhibition data yielded the K_i values summarized in Table 4. The noncompetitive pattern observed with SAH versus P-DME indicates formation of an E·SAH·P-DME dead-end complex. The inhibition constants for SAH were ~5-fold lower than the IC_{50} values reported for the *Plasmodium* PEAMT (*13*). Using phosphocholine, competitive inhibition patterns were observed versus each substrate (Figure 6C,D). The K_i values of phosphocholine for PMT-2 (Table 4) were comparable to the IC_{50} value (0.5 mM) described for the spinach enzyme (*11*).

Fluorescence Studies. To further test the proposed kinetic mechanism, fluorescence titrations were used to estimate the dissociation constants for the enzyme−ligand complexes. As shown in Figure 7A, P-DME and SAM quenched the fluorescence emission signal of PMT-2. Titration of the enzyme with P-DME and SAM (Figure 7B,C) yielded K_d values of 6.5 ± 0.6 and 1.2 ± 0.2 mM, respectively. Quenching of protein fluorescence emission was observed in titrations of PMT-2 using phosphocholine and SAH with dissociation constants of 7.3 ± 0.9 mM and 57 ± 10 μM, respectively.

DISCUSSION

Parasitic organisms, either protozoans or nematodes, are a major cause of disease worldwide (*15*, *16*). Ultimately, the development of drugs targeting pathways that differ between the parasite and host species offers a strategy for controlling these organisms. *C. elegans* is a model system for studying the biology of these metabolic pathways and the biochemistry of the enzymes catalyzing different reactions in target pathways. Since *Plasmodium* and nematodes synthesize phosphatidylcholine, a major phospholipid in the membranes of eukaryotes, using a metabolic pathway that differs from the biosynthetic pathway used in mammals, the PEAMTs are potential targets for the development of antiprotozoan and nematicidal compounds of medicinal and agricultural value (*15*). Understanding the biological function of these enzymes and establishing their kinetic mechanism are essential steps toward elucidating the PEAMT chemical mechanism and for inhibitor design.

Although related by sequence similarity, the plant, *Plasmodium*, and nematode PEAMTs catalyzing phosphocholine synthesis vary in the organization of their methyltransferase domains (Figure 2). The plant PEAMTs are single polypeptide molecules containing two tandem methyltransferase domains, each defined by a conserved set of sequence motifs (*12*−*14*). Generation of a truncated spinach PEAMT variant lacking the C-terminal domain demonstrated that the N-terminal methyltransferase domain catalyzes only the initial methylation of phosphoethanolamine to P-MME, suggesting

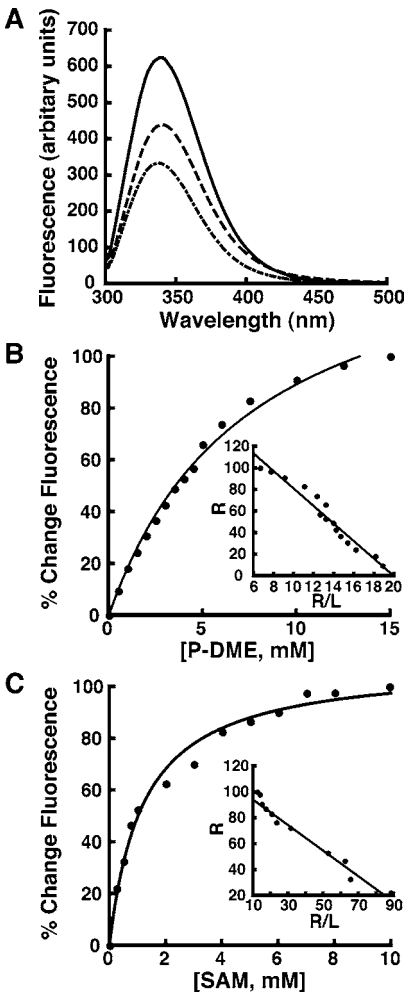

FIGURE 7: Fluorescence titration experiments. (A) Emission spectra of PMT-2 in the absence and presence of ligands. Emission spectra for PMT-2 (—) and the enzyme in the presence of 2 mM SAM (– – –) or 10 mM P-DME (-·-) are shown. All spectra were recorded as described in Experimental Procedures. (B and C) Determination of the K_d values for P-DME (B) and SAM (C). Data are plotted as the percentage of fluorescence change vs ligand concentration. The inset graph shows a linear transformation of the titration data, where R is the change in fluorescence upon ligand addition.

that the C-terminal methyltransferase domain performs the next two methylation reactions to yield phosphocholine (*13*). In contrast, the PEAMT from the malarial parasite *P. falciparum* is half the length of the plant enzymes and consists of a single methyltransferase domain that catalyzes the three-step methylation of phosphoethanolamine to phosphocholine (*15*, *16*). *C. elegans* adopted a third scheme for PEAMT-mediated phosphocholine synthesis.

The PEAMT from *C. elegans* described here is similar in amino acid length to the plant enzymes but retains only the C-terminal methyltransferase domain. Examination of the methyltransferase consensus motifs in the N-terminus of PMT-2 suggests a loss of function for this domain. As shown, PMT-2 uses P-MME and P-DME as substrates to generate P-DME and phosphocholine, respectively (Figure 4B). This is consistent with the proposed role of the C-terminal methyltransferase domain in the plant PEAMT (*13*, *14*). Interestingly, a second PEAMT-like gene[2] is present in *C. elegans* (gene, *pmt-1*; protein, PMT-1) and encodes a protein that only methylates phosphoethanolamine to P-MME.[3] The sequence of PMT-1 is 12% identical with that of PMT-2 but is more homologous (~25% identical sequence) with the N-terminal methyltransferase domains of the plant PEAMT.[3] Thus, in *C. elegans*, it is likely that gene duplication and divergence of the two PEAMT sequences into enzymes performing the initial and subsequent methylation reactions, respectively, occurred.

Disruption of endogenous *pmt-2* gene expression by feeding RNAi tested if the gene product is required for survival of *C. elegans* and if the protein is a potential nematicidal target. The dsRNA used in this study was designed to minimize the chance of off-target effects. Since the two *C. elegans* PEAMTs (PMT-1 and PMT-2) are 12% identical in sequence and extensive database searching using the *pmt-2* gene failed to detect the *pmt-1* gene or other related genes in *C. elegans*, the likelihood of cross-reactivity is minimal. In these experiments, *C. elegans* L1 and dauer larva grown in the presence of *E. coli* expressing dsRNA from the *pmt-2* gene yielded P0 sterility. Likewise, feeding RNAi to L4 larva resulted in arrested development and lethality in the F1 L1/L2 larva. The observed phenotypes are similar to those reported in RNAi experiments targeting phosphatidylcholine metabolism in *C. elegans* that resulted in drastic reductions in fertility, which is consistent with the role of phosphatidylcholine in embryo development (*36*). If the observed essential role in *C. elegans* is conserved in parasitic nematodes, such as *M. javanica*, *M. chitwoodi*, *M. incognita*, *G. rostochiensi*, *A. suum*, and *An. ceylanicum*, then inhibition of PMT-2 may be a viable nematicidal strategy.

Chemical complementation of the RNAi-mediated *pmt-2* phenotype provides information about the biological function of the protein. Growing *C. elegans* in media supplemented with choline reversed the *pmt-2* RNAi-mediated phenotype; however, chemical rescue of the phenotype did not occur in media supplemented with ethanolamine, monomethylethanolamine, or dimethylethanolamine (Table 1 and Figure 3). Providing choline bypasses the PEAMT pathway and allows direct entry of the metabolite into the Kennedy pathway in *C. elegans* (*37*). This indicates that the biological activity of PMT-2 is upstream from the entry of phosphocholine into the Kennedy pathway and is required for the utilization of P-MME and P-DME. The in vivo results correspond with the substrate specificity determined with the purified recombinant enzyme.

As described in Results, the steady-state kinetic properties of PMT-2 with SAM as a substrate are similar to those reported for the spinach, wheat, and *Plasmodium* enzymes (*13*–*15*), but the activity of any PEAMT has previously not been determined using P-MME or P-DME as a substrate. Comparison of the turnover rates of PMT-2 and the PEAMT from *Plasmodium* produced a 500-fold difference. Since the *Plasmodium* enzyme was assayed using phosphoethanolamine and not P-MME or P-DME, the first methylation reaction may be rate-limiting compared to the two subsequent reactions of phosphocholine synthesis.

The kinetic mechanism of PMT-2 was examined using initial velocity studies, analysis of product inhibition patterns, and ligand binding titrations. Overall, the results of these

[3] K. M. Brendza and W. Haakenson, unpublished data.

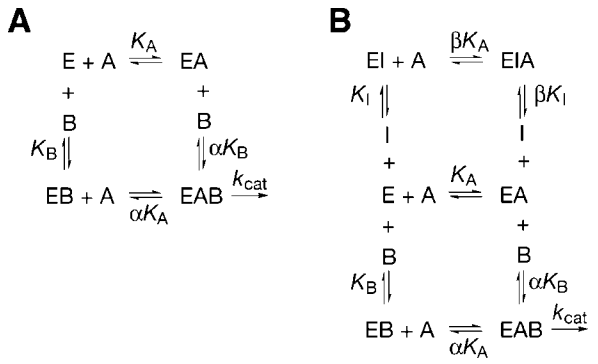

FIGURE 8: Model for a random sequential mechanism. (A) Chemical equilibria without inhibitor. (B) Chemical equilibria in the presence of an inhibitor (SAH) that forms a dead-end complex with a substrate (P-MME or P-DME).

experiments indicate that PMT-2 uses a random sequential kinetic mechanism for the synthesis of phosphocholine (Figure 8A). To distinguish between the three possible kinetic mechanisms describing a two-substrate to two-product or bi-bi reaction, reaction rates were determined using a matrix of SAM and P-DME concentrations (*29*, *30*, *34*). Because the initial velocity line patterns all intersect (Figure 5), a possible ping-pong mechanism was eliminated from further consideration. Comparison of the global fitting analysis of the data to equations for either ordered or random sequential mechanisms indicates that a random mechanism best describes the observed data obtained with PMT-2 (Table 3). The fitted parameters of V_{max}, K_{SAM}, and K_{P-DME} are similar to the experimentally observed turnover rate and the binding constants determined for each substrate by fluorescence titration. Likewise, the calculated values of αK_{SAM} and αK_{P-DME} were comparable to the observed K_m values for each substrate. The interaction factor ($\alpha = 0.3$) implies that binding of either substrate to the enzyme increases the binding affinity 3-fold for the second substrate.

Product inhibition experiments provide additional evidence for a random sequential kinetic mechanism for PMT-2. The observed product inhibition patterns (Figure 6 and Table 4) are not those expected for an ordered bi-bi mechanism but match the inhibition patterns expected for a random sequential mechanism (*35*). In a random bi-bi mechanism, if no dead-end complexes form between the product inhibitor and a substrate, then all the product inhibition patterns exhibit competitive inhibition profiles (*35*); however, noncompetitive inhibition occurs in the presence of abortive complexes. Since inhibition of PMT-2 by SAH was competitive versus SAM and noncompetitive versus P-DME, a dead-end complex forms between this product and P-DME (Figure 8B). In addition, the K_i value of SAH suggests that PMT-2 may be regulated by feedback inhibition, since the binding affinity for this product is higher than that for SAM. This also appears to be true for the *Plasmodium* enzyme, in which the estimated IC_{50} value for SAH was roughly 3−5-fold lower than the K_m value for SAM (*15*). The variation in binding constants between SAM and SAH in other SAM-dependent methyltransferases is attributed to the difference of binding the sulfonium group of SAM in a hydrophobic environment (*38*).

Fluorescence titration experiments are also consistent with a random sequential kinetic mechanism for PMT-2 (Figure 7). Since the binding of either substrate quenches the fluorescence emission of PMT-2, the binding of one substrate does not require the presence of the other molecule. Similarly, SAH and phosphocholine bind to PMT-2 in the absence of the other product. Moreover, the experimentally determined K_d values for SAM and P-DME are comparable to estimates of these binding constants calculated by fitting the initial velocity data to the equation for a random sequential mechanism (Table 2). Likewise, the binding constants estimated by fluorescence titration and the inhibition constants for phosphocholine and SAH are similar. These results suggest that product release is random; however, the inability to assay the reverse reaction prevents accurate determination of this.

Taken together, the results of our initial velocity, product inhibition, and fluorescence titration studies indicate that PMT-2 uses a random sequential kinetic mechanism that resembles those reported for catechol *O*-methyltransferase, arylamine *N*-methyltransferase, and glutamylmethyltransferase (*39*−*41*). Conflicting results describe ordered and random kinetic mechanisms for the mammalian phosphatidylethanolamine *N*-methyltransferase (*42*, *43*). Studies on the PEAMT from *C. elegans* provide the kinetic basis for further structural and functional studies on the chemical reaction mechanism of PEAMT, which will be valuable for information for inhibitor screening and design.

Acknowledgment. We thank Brandi Chiapelli for assisting with the RNAi rescue experiments.

REFERENCES

1. Carman, G. M., and Henry, S. A. (1989) Phospholipid biosynthesis in yeast, *Annu. Rev. Biochem. 58*, 635−669.
2. Kent, C. (1995) Eukaryotic phospholipid biosynthesis, *Annu. Rev. Biochem. 64*, 314−343.
3. Lykidis, A., and Jackowski, S. (2001) Regulation of mammalian cell membrane biosynthesis, *Prog. Nucl. Acid Res. Mol. Biol. 65*, 361−393.
4. Sohlenkamp, C., Lopez-Lara, I. M., and Geiger, O. (2003) Biosynthesis of phosphatidylcholine in bacteria, *Prog. Lipid Res. 42*, 115−162.
5. Kanipes, M. I., and Henry, S. A. (1997) The phospholipid methyltransferases in yeast, *Biochim. Biophys. Acta 1348*, 138−141.
6. Vance, D. E., Walkey, C. J., and Cui, Z. (1997) Phosphotidylethanolamine methyltransferase from liver, *Biochim. Biophys. Acta 1348*, 142−150.
7. Mudd, S. H., and Datko, A. H. (1986) Phosphoethanolamine bases as intermediates in phosphatidylcholine synthesis in *Lemna*, *Plant Physiol. 82*, 126−135.
8. Datko, A. H., and Mudd, S. H. (1988) Phosphatidylcholine synthesis: Differing patterns in soybean and carrot, *Plant Physiol. 88*, 854−861.
9. Datko, A. H., and Mudd, S. H. (1988) Enzymes of phosphatidylcholine synthesis in *Lemna*, soybean, and carrot, *Plant Physiol. 88*, 1338−1348.
10. Bolognese, C. P., and McGraw, P. (2000) The isolation and characterization in yeast of a gene for *Arabidopsis S*-adenosylmethionine:phospho-ethanolamine *N*-methyltransferase, *Plant Physiol. 124*, 1800−1813.
11. Nuccio, M. L., Ziemak, M. J., Henry, S. A., Weretilnyk, E. A., and Hanson, A. D. (2000) cDNA cloning of phosphoethanolamine *N*-methyltransferase from spinach by complementation in *Schizosaccharomyces* pombe and characterization of the recombinant enzyme, *J. Biol. Chem. 275*, 14095−14101.
12. Charron, J. B., Breton, G., Danyluk, J., Muzac, I., Ibrahim, R. K., and Sarhan, F. (2002) Molecular and biochemical characterization of a cold-regulated phosphoethanolamine *N*-methyltransferase from wheat, *Plant Physiol. 129*, 363−373.
13. Pessi, G., Kociubinski, G., and Mamoun, C. B. (2004) A pathway for phosphatidylcholine biosynthesis in *Plasmodium falciparum*

involving phosphoethanolamine methylation, *Proc. Natl. Acad. Sci. U.S.A. 101*, 6206−6211.
14. Pessi, G., Choi, J. Y., Reynolds, J. M., Voelker, D. R., and Mamoun, C. B. (2005) *In vivo* evidence for the specificity of *Plasmodium falciparum* phosphoethanolamine methyltransferase and its coupling to the Kennedy pathway, *J. Biol. Chem. 280*, 12461−12446.
15. Chaudhary, K., and Roos, D. S. (2005) Protozoan genomics for drug discovery, *Nat. Biotechnol. 9*, 1089−1091.
16. Nirmalan, N., Sims, P. F., and Hyde, J. E. (2004) Quantitative proteomics of the human malaria parasite *Plasmodium falciparum* and its application to studies of development and inhibition, *Mol. Microbiol. 52*, 1187−1199.
17. Sherman, I. W. (1979) Biochemistry of *Plasmodium*, *Microbiol. Rev. 43*, 453−495.
18. Ancelin, M. L., Calas, M., Bompart, J., Cordina, G., Martin, D., Ben Bari, M., Jei, T., Druilhe, P., and Vial, H. J. (1998) Antimalarial activity of 77 phospholipid polar head analogs: Close correlation between inhibition of phospholipid metabolism and *in vitro Plasmodium falciparum* growth, *Blood 91*, 1426−1437.
19. Calas, M., Ancelin, M. L., Cordina, G., Portefaix, P., Piquet, G., Vidal-Saihan, V., and Vial, H. (2000) Antimalarial activity of compounds interfering with *Plasmodium falciparum* phospholipid metabolism: Comparison between mono- and bisquaternary ammonium salts, *J. Med. Chem. 43*, 505−516.
20. Wengelnik, K., Vidal, V., Ancelin, M. L., Cathiard, A. M., Morgat, J. L., Kocken, C. H., Calas, M., Herrera, S., Thomas, A. W., and Vial, H. J. (2002) A class of potent antimalarials and their specific accumulation in infected erythrocytes, *Science 295*, 1311−1314.
21. Roggero, R., Zufferey, R., Minca, M., Richier, E., Calas, M., Vial, H., and Ben Mamoun, C. (2004) Unraveling the mode of action of the antimalarial choline analog G25 in *Plasmodium falciparum* and *Saccharomyces cerevisiae*, *Antimicrob. Agents Chemother. 48*, 2816−2824.
22. Tabara, H., Grishok, A., and Mello, C. C. (1998) RNAi in *C. elegans*: Soaking in the genome sequence, *Science 282*, 430−431.
23. Kamath, R. S., Martinez-Campos, M., Zipperlen, P., Fraser, A. G., and Ahringer, J. (2001) Effectiveness of specific RNA-mediated interference through ingested double-stranded RNA in *Caenorhabditis elegans*, *GenomeBiology 2*, RESEARCH0002.
24. Timmons, L., and Fire, A. (1998) Specific interference by ingested dsRNA, *Nature 395*, 854.
25. Emanuele, J. J., Jin, H., Yanchunas, J., and Villafranca, J. J. (1997) Evaluation of the kinetic mechanism of *Escherichia coli* uridine diphosphate-*N*-acetylmuramate:L-alanine ligase, *Biochemistry 36*, 7264−7271.
26. Brekken, D. L., and Phillips, M. A. (1998) *Trypanosoma brucei* γ-glutamylcysteine synthetase. Characterization of the kinetic mechanism and the role of Cys-319 in cystamine inactivation, *J. Biol. Chem. 273*, 26317−26322.
27. Jez, J. M., Cahoon, R. E., and Chen, S. (2004) *Arabidopsis thaliana* glutamate-cysteine ligase: Functional properties, kinetic mechanism, and regulation of activity, *J. Biol. Chem. 279*, 33463−33470.
28. Jez, J. M., and Cahoon, R. E. (2004) Kinetic mechanism of glutathione synthetase from *Arabidopsis thaliana*, *J. Biol. Chem. 279*, 42726−42731.
29. Segal, I. H. (1975) *Enzyme Kinetics: Behavior and Analysis of Rapid Equilibrium and Steady-State Enzyme Systems*, John Wiley and Sons, Inc., New York.
30. Cleland, W. W. (1979) Statistical analysis of enzyme kinetic data, *Methods Enzymol. 63*, 103−138.
31. Kagan, R. M., and Clarke, S. (1994) Widespread occurrence of three sequence motifs in diverse *S*-adenosylmethionine-dependent methyltransferases suggests a common structure for these enzymes, *Arch. Biochem. Biophys. 310*, 417−427.
32. Shields, D. J., Altarejos, J. Y., Wang, X., Agellon, L. B., and Vance, D. E. (2003) Molecular dissection of the *S*-adenosylmethionine-binding site of phosphatidylethanolamine *N*-methyltransferase, *J. Biol. Chem. 278*, 35826−35836.
33. Gee, P., and Kent, C. (2003) Multiple isoforms of choline kinase from *Caenorhabditis elegans*: Cloning, expression, purification, and characterization, *Biochim. Biophys. Acta 1648*, 33−42.
34. Fromm, H. J. (1979) Summary of kinetic reaction mechanisms, *Methods Enzymol. 63*, 42−53.
35. Rudolph, F. B. (1979) Product inhibition and adortive complex formation, *Methods Enzymol. 63*, 411−436.
36. Lochnit, G., Bongaarts, R., and Geyer, R. (2005) Searching new targets for anthelmintic strategies: Interference with glycosphingolipid biosynthesis and phosphorylcholine metabolism affects development of *Caenorhabditis elegans*, *Int. J. Parasitol. 35*, 911−923.
37. Lochnit, G., and Geyer, R. (2003) Evidence for the presence of the Kennedy and Bremer-Greenberg pathways in *Caenorhabditis elegans*, *Acta Biochim. Pol. 50*, 1239−1243.
38. Van Lanen, S. G., and Iwata-Reuyl, D. (2003) Kinetic mechanism of the tRNA-modifying enzyme *S*-adenosylmethionine:tRNA ribosyltransferase-isomerase (QueA), *Biochemistry 42*, 5312−5320.
39. Coward, J. K., Slisz, E. P., and Wu, F. Y. (1973) Kinetic studies on catechol O-methyltransferase: Product inhibition and the nature of the catechol binding site, *Biochemistry 12*, 2291−2297.
40. Lyon, E. S., and Jakoby, W. B. (1982) Arylamine *N*-methyltransferase: Methylation of the indole ring, *J. Biol. Chem. 257*, 7531−7535.
41. Simms, S. A., and Subbaramaiah, K. (1991) The kinetic mechanism of *S*-adenosyl-L-methionine:glutamylmethyltransferase from *Salmonella typhimurium*, *J. Biol. Chem. 266*, 12741−12746.
42. Ridgway, N. D., and Vance, D. E. (1988) Kinetic mechanism of phosphatidylethanolamine *N*-methyltransferase, *J. Biol. Chem. 263*, 16864−16871.
43. Reitz, R. C., Mead, D. J., Bjur, R. A., Greenhouse, A. H., and Welch, W. H. (1989) Phosphatidylethanolamine *N*-methyltransferase in human red blood cell membrane preparations: Kinetic mechanism, *J. Biol. Chem. 264*, 8097−8106.

BI060199D